Single and Dual Polarization InGaAs Optical Coherent Receivers for Coherent LADARs

Abhay M Joshi and Shubhashish Datta
Discovery Semiconductors, Inc.
119 Silvia Street, Ewing, New Jersey 08628, USA
sdatta@discoverysemi.com

Abstract: We have manufactured single as well as dual polarization optical coherent receivers that comprise of InGaAs balanced receivers and an optical hybrid. The bandwidth of InGaAs balanced receivers is up to 20 GHz with a wavelength coverage of 1200 nm to 2200 nm. The single polarization coherent receiver contains two balanced receivers and a single polarization 90 degree optical hybrid; whereas the dual polarization coherent receiver contains four balanced receivers and a dual polarization 90 degree optical hybrid. The optical hybrids have limited wavelength coverage, mainly from 1530 nm to 1610 nm, and could be customized for 2000 nm operation. The InGaAs balanced receivers offer several features such as user-adjustable RF gain, bandwidth, and mode of operation (Automatic Gain Control [AGC] or Manual Gain Control). The AGC mode with a programmable differential voltage output up to 750 mV peak-to-peak compensates atmospheric fades and maximizes Effective Number of Bits (ENOBs) for backend digital signal processing.

Keywords: ultrafast photoreceiver, polarization diversity receiver, automatic gain control, coherent LADAR, extended InGaAs

1. Introduction

Laser radars (LADAR) illuminate a distant target and analyze the reflected or backscattered optical signal to ascertain its properties, such as location, velocity, and material composition. The received optical signals typically have low light levels and fluctuations induced by atmospheric fades, and are challenging to analyze with direct detection systems. Systems based on ultra-fast coherent receivers with automatic gain control, as shown in Fig. 1, enable shot noise-limited detection of amplitude, phase, and polarization of the received optical signal with a timing precision of tens of picoseconds.

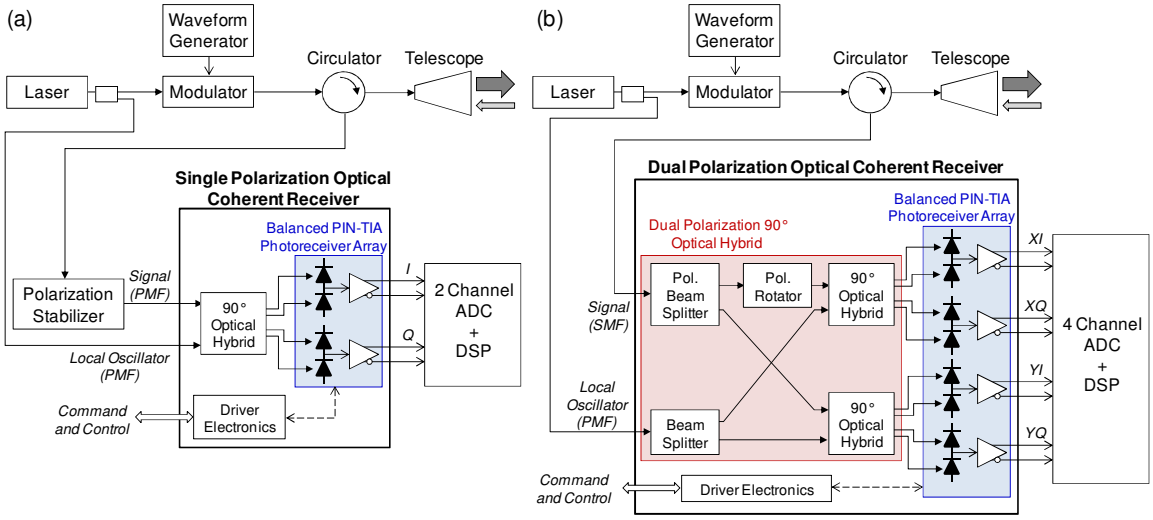

Figure 1. Block diagrams of coherent laser radar that incorporate (a) single polarization and (b) dual polarization ultra-fast coherent receivers having user-adjustable bandwidth and gain control.

The single polarization coherent receiver, which is comprised of two balanced receivers and a 90 degree optical hybrid, operates in conjunction with an external polarization stabilizer to mix the received optical signal with a local optical oscillator and demodulate it into in-phase (*I*) and quadrature phase (*Q*) components. This receiver, shown in Fig. 1a, is appropriate for applications such as Doppler LADARs that only require amplitude and phase analysis [1, 2].

In a dual polarization coherent receiver, shown in Fig. 1b, the received optical signal is first split into its orthogonal linear polarization states (*X* and *Y*) prior to demodulation into corresponding in-phase and quadrature phase components, namely *XI*, *XQ*, *YI*, and *YQ*. Such a receiver is necessary for polarization diversity LADARs that immunize the system to polarization fluctuations without requiring a polarization stabilizer. Additionally, dual polarization receiver enables polarimetry in LADARs, which is useful for material characterization [3].

Material characterization is further aided by multi-wavelength differential absorption laser radars (DIAL), which have been used for atmospheric sensing [4]. The ultra-fast InGaAs balanced receivers presented here have a broad wavelength coverage of 1200 nm to 2200 nm and are appropriate for such DIAL applications with a distance accuracy of ~1 cm. Both single and dual polarization optical hybrids currently have limited wavelength coverage, mainly from 1530 nm to 1610 nm, but have virtually unlimited bandwidth in the RF domain. These hybrids could be customized for 2000 nm operation.

We first describe the novel uncooled lattice-mismatched InP / InGaAs p-i-n photodiode technology that extends the ultra-fast operation from a traditional cut-off wavelength of 1650 nm to 2200 nm. These photodiodes enable using high-power 2 micron wavelength lasers that have been touted as a success story of NASA's Laser Risk Reduction Program for space-based atmospheric sensing [5]. We then narrate the balanced photoreceiver that combines a pair of InGaAs photodiodes with a differential transimpedance amplifier having a user-adjustable RF gain, automatic gain control with adjustable RF output amplitude, and adjustable bandwidth for matched filtering. Finally, the optical coherent receivers are described which can operate with an aggregate DC photocurrent of up to 16 mA for shot noise-limited detection.

2. Uncooled Lattice-Mismatched InP / InGaAs Photodiodes

Conventional InP / InGaAs photodiodes, commonly used in 1550 nm wavelength systems, utilize $In_{0.53}Ga_{0.47}As$ absorber layer that is lattice-matched to the InP substrate (lattice constant = 5.87 Å). The cut-off wavelength of these devices is limited to 1650 nm by the bandgap of $In_{0.53}Ga_{0.47}As$ material (Eg = 0.74 eV). In this work, we utilized a lower bandgap material, namely Indium-rich $In_{0.72}Ga_{0.28}As$ (Eg = 0.57 eV) as the absorber layer, to extend the photodiode's cut-off wavelength to 2200 nm at ambient room temperature. The epitaxial structure of the lattice-mismatched $In_{0.72}Ga_{0.28}As$ / InP photodiode is compared with the conventional lattice-matched $In_{0.53}Ga_{0.47}As$ / InP photodiode in Fig. 2.

The primary challenge in incorporating Indium-rich absorption layer is to minimize the dislocation defects that may arise from the lattice mismatch between $In_{0.72}Ga_{0.28}As$ (lattice constant = 5.94 Å) and the InP substrate. These defects act as generation-recombination centers and increase the photodiode's dark current. Also, these defects may provide interstitial sites for material impurities and elevate unintentional background doping level in intrinsic $In_{0.72}Ga_{0.28}As$ absorption layer [6]. As a result, larger reverse bias is needed in a material with higher defect density to achieve a targeted depletion width and device capacitance for ultra-fast operation. The photodiode structure shown in Fig. 2a utilizes n-doped graded $InAs_yP_{1-y}$ buffer layer that is lattice-matched to the (100) oriented, n^+-doped InP substrate in the bottom and the $In_{0.72}Ga_{0.28}As$ absorber on the top. This buffer layer contains compositionally abrupt interfaces that minimize the propagation of lattice defects into the subsequently grown intrinsic $In_{0.72}Ga_{0.28}As$ absorption layer. We have achieved uncooled 25 GHz photodiode operation with DC responsivity of ~0.9 A/W at 1550 nm wavelength and ~1.2 A/W at 2050 nm wavelength [7, 8].

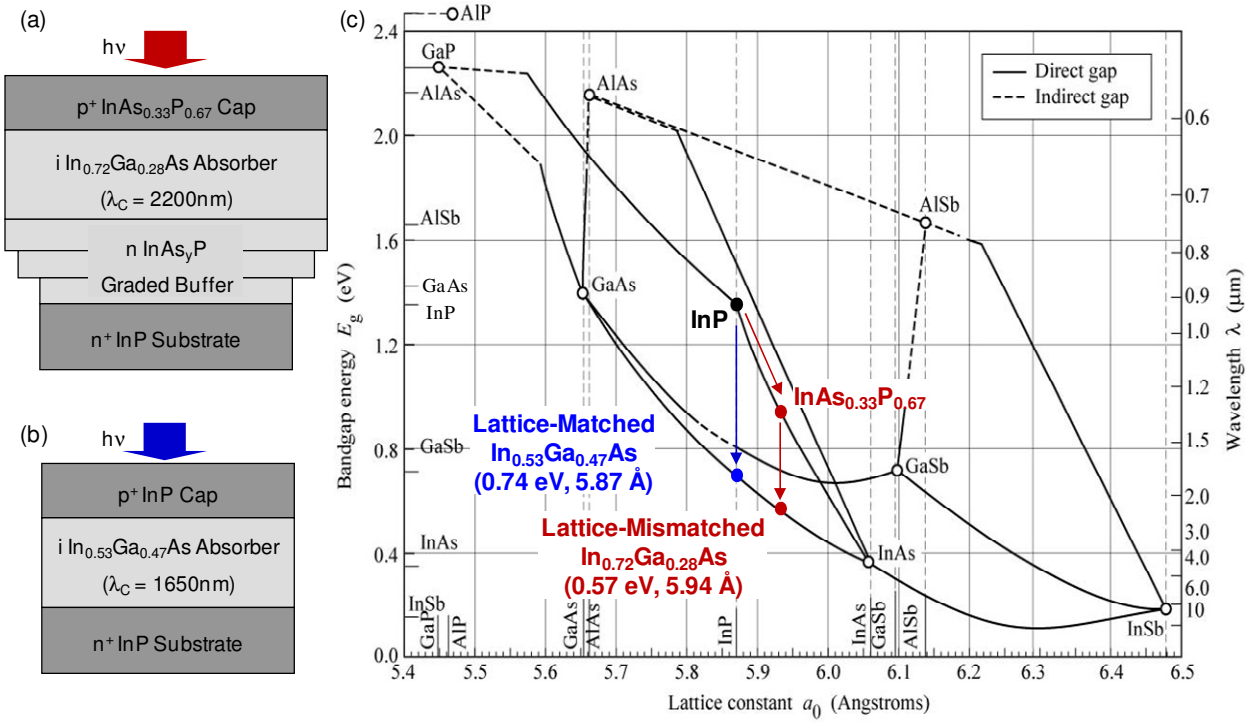

Figure 2. Epitaxial structure of (a) lattice-mismatched $In_{0.72}Ga_{0.28}As$ / InP photodiode used in this work is compared with (b) conventional lattice-matched $In_{0.53}Ga_{0.47}As$ / InP photodiode. (c) Bandgap and lattice constant of III-V semiconductors with materials of the two photodiode structures annotated.

3. Balanced Photoreceiver with Adjustable Gain and Bandwidth

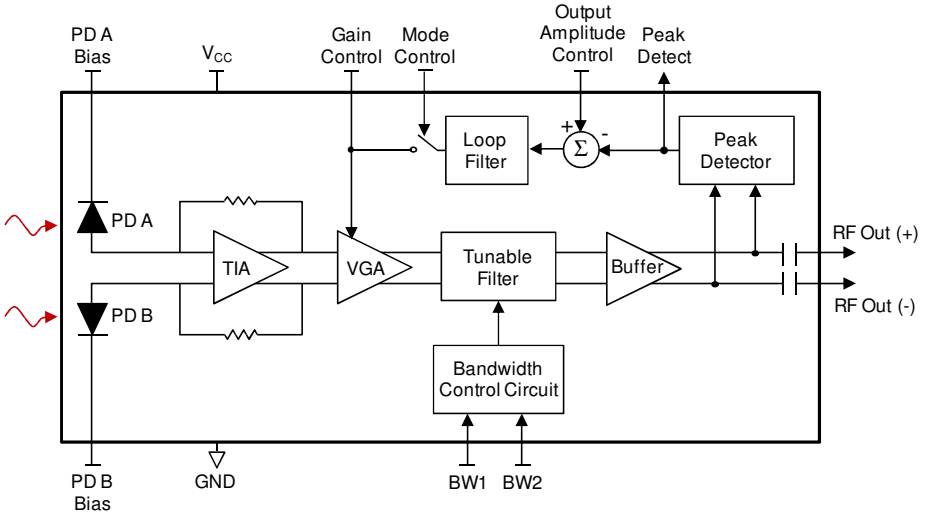

Figure 3. The block diagram of the balanced photoreceiver, incorporating two $In_{0.72}Ga_{0.28}As$ photodiodes (PD A and PD B), shows an open feedback loop for Manual Gain Control mode. The feedback loop can be closed using the "Mode Control" input for Automatic Gain Control mode.

The balanced photoreceiver is comprised of two 30 μm diameter $In_{0.72}Ga_{0.28}As$ photodiodes that are coupled to a differential amplifier, as shown in Fig 3. Beyond the usual advantages of balanced detection, such as cancellation of common-mode relative intensity noise (RIN) and suppression of second-order distortions, this device has several features to enhance its flexibility:

- The amplifier's transfer function can be chosen between seven settings by using two tri-state control signals, BW1 and BW2. As shown in Fig. 4a, the -3 dB bandwidth of the balanced photoreceiver can be optimized for specific applications. It should be noted that 18 GHz bandwidth corresponds to a time constant of 55 ps and a distance of 1.6 cm for light travelling in free space.
- The amplifier circuit incorporates a variable gain amplifier (VGA) following the input-stage trans-impedance amplifier (TIA) which allows adjusting the differential transimpedance up to 4600 Ω, as shown in Fig. 4b. Consequently, the differential conversion gain can be varied up to 5600 V/W for a photodiode responsivity of 1.2 A/W at 2050 nm wavelength. The input equivalent noise varies from 15 pA/√Hz to 38 pA/√Hz at the maximum gain setting (see Fig. 4c).
- The photoreceiver also contains a peak detection circuit that generates a voltage proportional to the peak-to-peak RF output amplitude and may be useful optimizing local oscillator power level in a coherent LADAR.
- The amplifier circuit can be operated in two modes, Manual Gain Control or Automatic Gain Control (AGC), which is determined by the "Mode Control" input. In the AGC mode, the feedback loop shown in Fig. 3 is closed and the peak detect signal is used internally to maintain a targeted peak-to-peak RF output amplitude, which can compensate for atmospheric fades. This targeted output amplitude can be chosen by the user up to 750 mV_{p-p} differential by using the "Output Amplitude Control" input and is sufficient to maximize Effective Number of Bits (ENOBs) for backend digital signal processing.

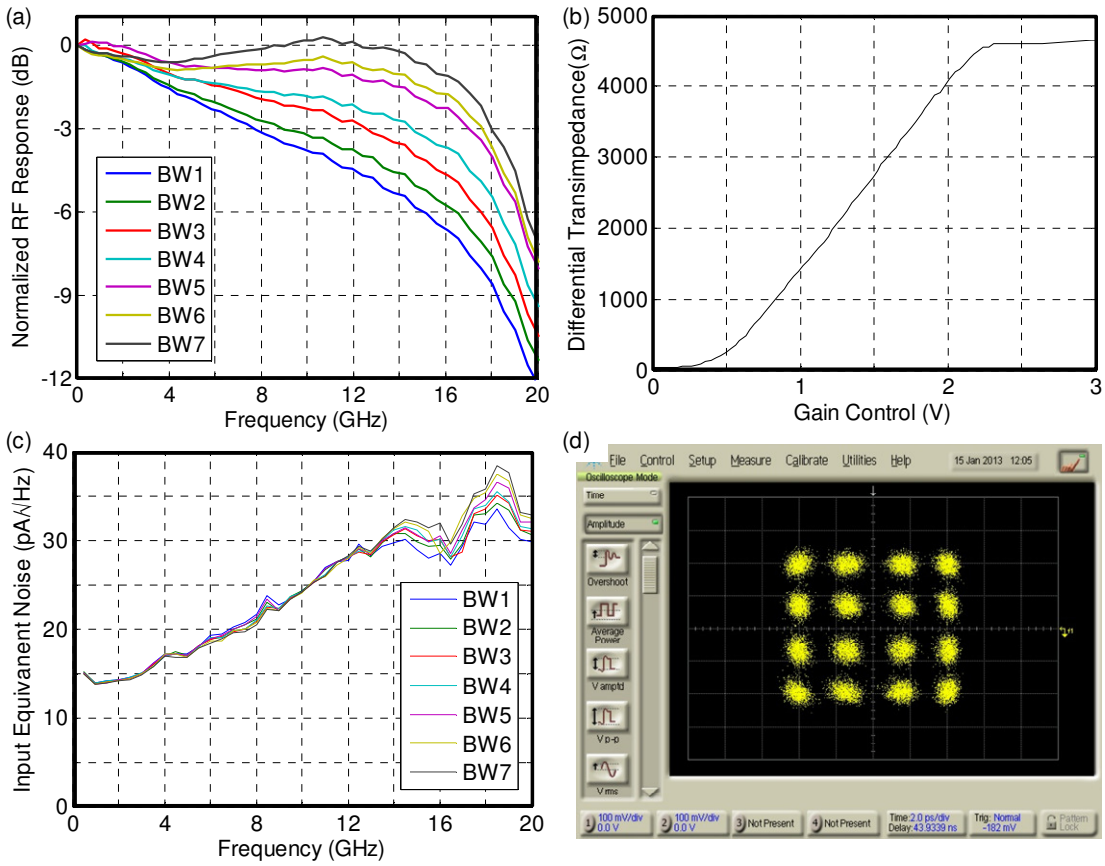

Figure 4. (a) Normalized RF response for seven user-adjustable bandwidth settings, (b) Differential transimpedance vs. gain control voltage, and (c) Input equivalent noise density at maximum gain setting of the $In_{0.72}Ga_{0.28}As$ balanced photoreceiver. (d) 16-QAM constellation having 12.5 Gbaud symbol rate for X-polarization of the dual-polarization coherent receiver shown in Fig. 1b.

4. Optical Coherent Receivers

The optical coherent receivers, shown in Fig. 1, incorporate these balanced photoreceivers integrated with single polarization and dual polarization 90 degree optical hybrids, as well as driver electronics for controlling the gain and bandwidth of the photoreceivers in an instrument format. Channel-to-channel symmetry of the optical hybrids and the balanced photoreceivers ensure a phase error within ±5° between in-phase and quadrature signals, and a maximum channel skew of 10 ps. This symmetry is exemplified by the 16-quadrature amplitude modulated (16-QAM) constellation shown in Fig. 4d, which was generated by co-plotting 4-level 12.5 Gbaud signals from *XI* and *XQ* channels of the dual-polarization coherent receiver shown in Fig. 1b. Similar 16-QAM constellation is obtained from the *YI* and *YQ* channels.

Each balanced photoreceiver can be operated at a maximum DC photocurrent of 2 mA per diode, which corresponds to an aggregate DC photocurrent of 8 mA for the single polarization device, and 16 mA for the dual polarization device. For a typical excess insertion loss of 3 dB in the optical hybrids, the coherent receivers can be operated at optical LO power levels of up to +13 dBm for the single polarization device, and +16 dBm for the dual polarization device, which is sufficient for shot noise-limited detection.

5. Conclusion

In summary, we have developed single and dual polarization ultra-fast coherent receivers that enable several key features in coherent LADARs, namely shot-noise limited detection of reflected or back-scattered optical signals with a distance accuracy of ~1 cm, polarimetry, compensation of atmospheric fades through automatic gain control, and large RF output signal to maximize the ENOBs for backend digital signal processing. These receivers are based on uncooled, lattice-mismatched InGaAs photodiode technology having wavelength coverage of 1200 nm to 2200 nm, which further enables utilizing high-power 2 micron wavelength lasers.

6. References

[1] S. Hannon, J. Alex, S. Henderson, P. Gatt, R. Stoneman, and D. Burns, "Agile multiple-pulse coherent lidar for range and micro-Doppler measurement," Proc. SPIE **3380**, 259-269 (1998).

[2] F. Amzajerdian and D. Pierrottet, "Fiber-based coherent LIDAR for target ranging, velocimetry, and atmospheric wind sensing," in Conference on Lasers and Electro-Optics/Quantum Electronics and Laser Science Conference and Photonic Applications Systems Technologies, Technical Digest (Optical Society of America, 2006), paper CPDB9.

[3] R. Neely, M. Hayman, R. Stillwell, J. Thayer, R. Hardesty, M. O'Neill, M. Shupe, and C. Alvarez, "Polarization LIDAR at Summit, Greenland, for the detection of cloud phase and particle orientation," J. Atmospheric Oceanic Tech. **30**, 1635-1655 (2013).

[4] G. Koch, B. Barnes, M. Petros, J. Beyan, F. Amzajerdian, J. Yu, R. Davis, S. Ismail, S. Vay, M. Kavaya, and U. Singh, "Coherent differential absorption lidar measurements of CO_2," Applied Optics **43**, 5092-5099 (2004).

[5] U. Singh, B. Walsh, J. Yu, M. Petros, M. Kavaya, T. Refaat, and N. Barnes, "Twenty years of Tm:Ho:YLF and LuLiF laser development for global wind and carbon dioxide active remote sensing," Optical Materials Express **5**, 828-837 (2015).

[6] A. Joshi, G. Olsen, S. Mason, M. Lange, and V. Ban, "Near-Infrared (1-3 μm) InGaAs Detectors and Arrays: Crystal Growth, Leakage Current, and Reliability," Proc. SPIE **1715**, 585-593 (1992).

[7] A. Joshi, "Developments in High Performance Photodiodes," IEEE Photonics Conf. 2012, invited paper MS1, San Francisco, CA, 23 – 27 September 2012.

[8] A. Joshi, S. Datta, and M. Lange, "2.2 micron, uncooled, InGaAs photodiodes, and balanced photoreceivers up to 25 GHz bandwidth," Proc. SPIE **8704**, 87042G1-8 (2013).

Acknowledgement

The authors thank NASA Goddard Space Flight Center for funding the development of lattice-mismatched InGaAs photodiodes, and especially Dr. Sachidananda Babu, Dr. Peter Shu, and Dr. Murzy Jhabvala for their support.